PERGAMON

International Journal of Solids and Structures 40 (2003) 1189–1202

INTERNATIONAL JOURNAL OF SOLIDS and STRUCTURES

www.elsevier.com/locate/ijsolstr

Finite element calculation of elastodynamic stress field around a notch tip via contour integrals

J.H. Chang *, D.J. Wu [1]

Department of Civil Engineering, National Central University, Chungli 32054, Taiwan

Received 30 January 2002; received in revised form 5 November 2002

Abstract

Direct computation of the mixed-mode dynamic asymptotic stress field around a notch tip is difficult because the mode I and mode II stresses are in general governed by different orders of singularity. In this paper, we propose a pair of elastodynamic contour integrals $J_{kR}(t)$. The integrals are shown to be path-independent in a modified sense and so they can be accurately evaluated with finite element solutions. Also, by defining a pair of generalized stress intensity factors (SIFs) $K_{\mathrm{I},\beta}(t)$ and $K_{\mathrm{II},\beta}(t)$, the relationship between $J_{kR}(t)$ and the SIF's is derived and expressed as functions of the notch angle β. Once the $J_{kR}(t)$-integrals are accurately computed, the generalized SIF's and, consequently, the asymptotic mixed-mode stress field can then be properly determined. No particular singular elements are required in the calculation. The proposed numerical scheme can be used to investigate the dynamic amplifying effect in the near-tip stress field.

Keywords: Notch tip; Mixed-mode elastodynamic stresses; Generalized stress intensity factors; Elastodynamic J_{kR}-integrals; Modified path-independence

1. Introduction

The modes I and II fracture states associated with a notch tip are in general governed by different orders of singularity, with the strength of singularity for mode II weaker than that of mode I. While numerous analytical studies on description of the quasi-static asymptotic singular stress behavior in the near-tip region have been performed (e.g. Williams, 1952; Bogy, 1972; Awaji et al., 1986; Peng, 1986, etc.), direct evaluation of the stress field with numerical schemes such as finite element method appears to be difficult due to the complicated mechanical state around the singular point.

For the special case when the singular point corresponds to a crack tip for linear elasticity, the mixed-mode near-tip characterizing parameters such as the stress intensity factors (SIF's) can be determined by combined use of the J_k-integrals ($k = 1, 2$) (Knowles and Sternberg, 1972; Budiansky and Rice, 1973). By

* Corresponding author. Tel.: +886-34-4255239; fax: +886-34-4252960.
E-mail address: t320001@cc.ncu.edu.tw (J.H. Chang).
[1] Research Assistant.

0020-7683/02/$ - see front matter © 2002 Elsevier Science Ltd. All rights reserved.
PII: S0020-7683(02)00645-5

definition, J_k are line integrals evaluated along a counterclockwise contour enclosing and shrinking onto the crack tip. For homogeneous media with traction-free crack surfaces, the first component J_1, also generally known as J, is path-independent. As regards J_2, the other component of J_k, the property of path-independence needs to be revised (Herrmann and Herrmann, 1981) and so the region near and at the crack tip is always involved in the calculation. Therefore, direct evaluation of J_2 from numerical solutions is difficult mainly owing to the singular mechanical behavior. To overcome this, approximate expressions for J_2, in conjunction with finite element solutions, were proposed for elastostatic (Eischen, 1987) and elastodynamic (Chang and Chen, 1998) conditions respectively. With these numerical schemes, J_2 can be accurately calculated without using any particular singular finite elements.

For a notch tip, however, the order of the stress singularity is generally different from that of the crack case (i.e., $r^{-1/2}$). As described, the symmetric (mode I) and antisymmetric (mode II) parts of the quasi-static near-tip asymptotic stress field are governed by different singular terms, with the orders of singularity depend upon the notch angle (Peng, 1986). In such a case, the conventional concept of SIF's and the J_k-integrals for crack problems is no longer valid. As a matter of fact, it was observed that the results of the J_k-integrals associated with a notch tip generally vanish. Therefore, instead of direct application of the J_k-integrals, a pair of alternative contour integrals termed J_{kR} for quasi-static problems were presented by the authors (Chang and Kang, 2002). By appropriately evaluating the J_{kR}-integrals, the asymptotic near-tip mixed-mode stress field can thus be consequently determined.

In this paper, a numerical procedure, incorporated with the finite element method, is developed for calculation of the elastodynamic asymptotic mixed-mode stress field for plane elastic problems containing a stationary notch tip. Since the J_k-integrals are not feasible for use in such problems, the formulation is based on the concept of the alternative elastodynamic parameters J_{kR}. With the numerical scheme, the generalized dynamic SIF's associated with the notch tip can be calculated. This is an extension of the aforementioned earlier work conducted by the authors on the corresponding quasi-static problems. No particular singular elements are used in the calculations.

2. The elastodynamic asymptotic stress field

Consider a homogeneous elastic body in a 2-D field, containing a stationary notch of arbitrary angle β (Fig. 1). The body is subjected to a system of dynamic loads and reaches its current deformed state at a specific time t. A local coordinate system originating at the notch tip O is introduced, with the notch angle being bisected by the (negative) x_1-axis. The stress field in the vicinity of a notch tip for the quasi-static case has been studied in the authors' previous work (Chang and Kang, 2002). Here, by taking the Airy stress function employed by Williams (1952) and considering the condition when the notch edges are traction-free, the elastodynamic asymptotic stress field in the immediate neighborhood of the notch tip can be expressed in terms of the following separable forms as functions of the notch angle

$$\sigma_r(r,\theta;\beta;t) = r^{\lambda 1}\frac{K_{\mathrm{I},\beta}(t)}{(2\pi-\beta)^{1/2}}[f_1(\beta)\cos\lambda_1\theta + g_1(\beta)\cos(\lambda_1+2)\theta] + r^{\lambda 2}\frac{K_{\mathrm{II},\beta}(t)}{(2\pi-\beta)^{1/2}}[h_1(\beta)\sin\lambda_2\theta + p_1(\beta)\sin(\lambda_2+2)\theta] \tag{1}$$

$$\sigma_\theta(r,\theta;\beta;t) = r^{\lambda 1}\frac{K_{\mathrm{I},\beta}(t)}{(2\pi-\beta)^{1/2}}[f_2(\beta)\cos\lambda_1\theta + g_2(\beta)\cos(\lambda_1+2)\theta] + r^{\lambda 2}\frac{K_{\mathrm{II},\beta}(t)}{(2\pi-\beta)^{1/2}}[h_2(\beta)\sin\lambda_2\theta + p_2(\beta)\sin(\lambda_2+2)\theta] \tag{2}$$

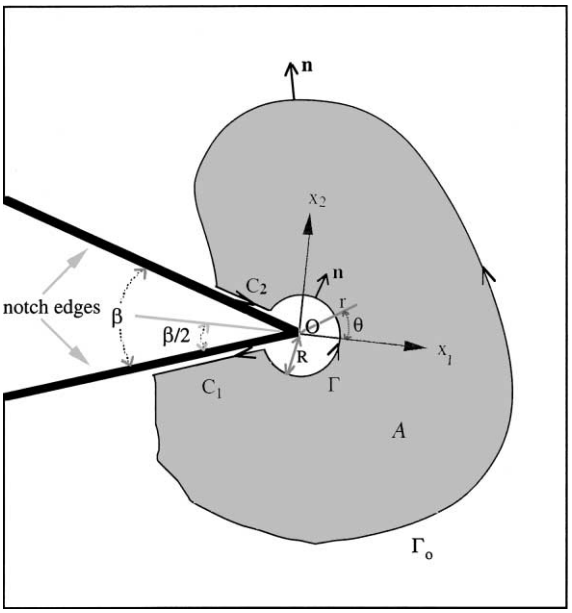

Fig. 1. An elastic body in a 2-D field, containing a stationary notch of angle β.

$$\tau_{r\theta}(r,\theta;\beta;t) = r^{\lambda 1}\frac{K_{\mathrm{I},\beta}(t)}{(2\pi-\beta)^{1/2}}[f_3(\beta)\sin\lambda_1\theta + g_3(\beta)\sin(\lambda_1+2)\theta] + r^{\lambda 2}\frac{K_{\mathrm{II},\beta}(t)}{(2\pi-\beta)^{1/2}}[h_3(\beta)\cos\lambda_2\theta + p_3(\beta)\cos(\lambda_2+2)\theta] \tag{3}$$

where (r,θ) denote the polar components of the local coordinate and $-(\pi-\beta/2)\leqslant\theta\leqslant(\pi-\beta/2)$. The orders of singularity, λ_1 and λ_2, are the smallest nontrivial real eigenvalues of the following pair of eigen equations

$$\sin[(\lambda+1)(2\pi-\beta)] \pm (\lambda+1)\sin\beta = 0 \tag{4}$$

The values of λ_1 and λ_2 are presented in Fig. 2 as functions of β, with $\lambda_2 \geqslant \lambda_1 \geqslant -0.5$. Also, the dimensionless coefficients f_i, h_i, g_i, and p_i ($i = 1, 2, 3$) are explicit functions of β and sketched in Fig. 3(a) and (b).

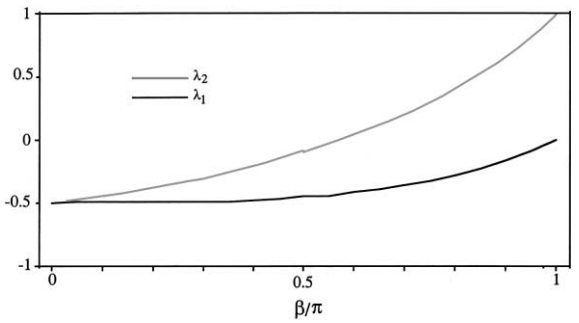

Fig. 2. The values of λ_1 and λ_2, as functions of the notch angle β.

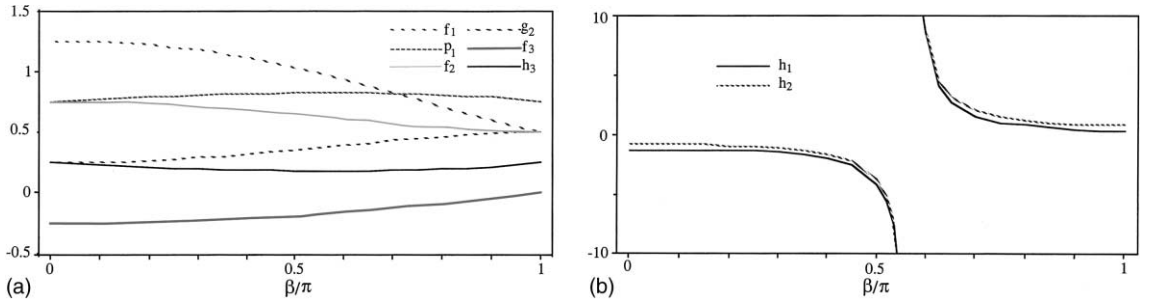

Fig. 3. (a) The variations of f_i, h_3, g_i, and p_i ($i = 1, 2, 3$) with respect to β. (b) The variations of h_1 and h_2 with respect to β.

The values of h_1 and h_2 become relatively large and change signs at $\beta \approx 0.57\pi$. In spite of such discontinuity of h_1 and h_2, the stress components σ_r and σ_θ still appear as continuous functions of β since the function $\sin \lambda_2\theta$ vanishes and changes signs at this specific value of β. Note that the orders of singularity and the corresponding angular functions are identical to those of the quasi-static case.

In the near-tip stress field, the generalized elastodynamic stress intensity factors for an arbitrary notch angle β at time t, denoted $K_{\mathrm{I},\beta}(t)$ and $K_{\mathrm{II},\beta}(t)$, can be defined as

$$K_{\mathrm{I},\beta}(t) \equiv \lim_{r\to 0}(2\pi-\beta)^{1/2} r^{-\lambda 1}\sigma_\theta(r,0;\beta;t) \tag{5}$$

$$K_{\mathrm{II},\beta}(t) \equiv \lim_{r\to 0}(2\pi-\beta)^{1/2} r^{-\lambda 2}\tau_{r\theta}(r,0;\beta;t) \tag{6}$$

These elastodynamic SIF's account for the strength of stress singularity in the near-tip region. They are undetermined constants, dependent upon the far-field loading and geometric conditions.

It is shown in Eqs. (1)–(3) that the mode I (symmetric) and mode II (antisymmetric) near-tip stress components are in general governed by different orders of singularity, except for the special case when $\beta = 0$ (i.e., the crack problem, with $\lambda_1 = \lambda_2 = -0.5$). It is observed that the strength of singularity for mode II stresses is essentially weaker than those of mode I. Furthermore, for notch angles greater than 0.57π (approximately), the problem considered has bounded mode II stresses in the near-tip region. Such singular behavior is well consistent with that described by Peng (1986).

3. The elastodynamic J_{kR}-integrals for a notch tip

As an analog to the conventional elastodynamic J_k-integrals for crack problems (Nishioka and Atluri, 1983), the corresponding contour integrals for a notch tip can be defined as

$$J_k(t) = \lim_{\Gamma\to 0}\int_\Gamma \left[(W+T)n_k - \sigma_{ij}n_j\left(\frac{\partial u_i}{\partial x_k}\right)\right]\mathrm{d}s \qquad k = 1,2 \tag{7}$$

where W is the strain energy density of the material, T is the kinetic energy density, σ_{ij} and u_i are the Cartesian components of the stress tensor and the displacement vector, n_j are the Cartesian components of outward unit vector normal to Γ (as shown in Fig. 1), and s is the arc length along the contour. The path of integration, Γ, is defined as a counterclockwise contour encircling and shrinking onto the tip of the notch O (this limiting case is not shown in Fig. 1).

For the special case when $\beta = 0$, the integration in Eq. (7) results in a pair of finite-valued solutions for $J_1(t)$ and $J_2(t)$. Physically, they can be identified as the elastodynamic energy release rates for a stationary

crack as the crack advances along and perpendicular to its original orientation respectively. As well demonstrated for both static (e.g. Hellen and Blackburn, 1975) and dynamic (Nishioka and Atluri, 1983) cases, J_k can be related to the SIF's as

$$J_1(t) = \frac{\Lambda}{E}\left[K_{\mathrm{I},0}^2(t) + K_{\mathrm{II},0}^2(t)\right] \tag{8}$$

$$J_2(t) = -\frac{2\Lambda}{E}K_{\mathrm{I},0}(t)K_{\mathrm{II},0}(t) \tag{9}$$

where $\Lambda = 1$ (for plane stress) or $1 - v^2$ (for plane strain), E is the Young's modulus, and v is the Poisson's ratio. The above equations show that, not only can the integrals be employed explicitly as the energy fracture parameters for plane crack problems, they can also be used to evaluate the SIF's $K_{\mathrm{I},0}(t)$ and $K_{\mathrm{II},0}(t)$ at the crack tip. However, for notch problems with generally $\beta > 0$, the characteristic of finite values and the physical meanings of J_k are no longer valid. Also, the relationship between $J_k(t)$ and the generalized SIF's is still not obvious.

To investigate the behavior of $J_k(t)$ for a notch tip, we consider a properly chosen circular contour with center at the tip O and of arbitrarily small radius, say, r, as shown in Fig. 1. Although not explicitly shown here, it is implied by Eqs. (1)–(3) that the velocity field in the near-tip region is governed by the two dominant terms $r^{\lambda 1+1}$ (mode I) and $r^{\lambda 2+1}$ (mode II). This indicates that the corresponding kinetic energy density T is non-singular since it is at least of the order of $\mathrm{O}(r^{2\lambda 1+2})$, with $\lambda_1 \geqslant -0.5$. Therefore, the contribution from T in Eq. (7) is relatively negligible as Γ shrinks onto the notch tip O, i.e.,

$$J_k(t) \to \lim_{\Gamma\to 0}\int_{\Gamma}\left[Wn_k - \sigma_{ij}n_j\left(\frac{\partial u_i}{\partial x_k}\right)\right]\mathrm{d}s \qquad k = 1, 2 \tag{10}$$

Substituting Eqs. (1)–(3), together with the asymptotic displacement field, into Eq. (10) and taking integration along this path counterclockwisely, we then have

$$J_1(t) = \lim_{r\to 0}\frac{\Lambda}{E}\left[r^{2\lambda_1+1}a(\beta)K_{\mathrm{I},\beta}^2(t) + r^{2\lambda_2+1}b(\beta)K_{\mathrm{II},\beta}^2(t)\right] \tag{11}$$

$$J_2(t) = \lim_{r\to 0} -\frac{2\Lambda}{E}r^{\lambda_1+\lambda_2+1}c(\beta)K_{\mathrm{I},\beta}(t)K_{\mathrm{II},\beta}(t) \tag{12}$$

where $a(\beta)$, $b(\beta)$, and $c(\beta)$ are dimensionless functions of β and their variations with respect to β are shown in Fig. 4. It is observed that, in addition to $K_{\mathrm{I},\beta}(t)$ and $K_{\mathrm{II},\beta}(t)$, three extra terms (i.e., $r^{2\lambda 1+1}$, $r^{2\lambda 2+1}$, and

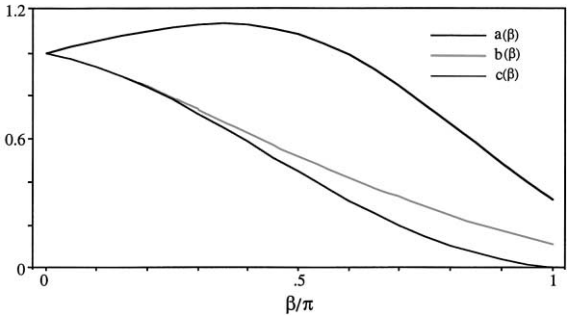

Fig. 4. The variations of a, b, and c with respect to β.

$r^{\lambda 1+\lambda 2+1}$) are contained in Eqs. (11) and (12). With the presence of the three terms, we anticipate that the values of $J_k(t)$ vanish as the limiting condition $r \to 0$ by definition. Note that, when $\beta = 0$, the three terms become unity and the solutions of $J_k(t)$ reduce to Eqs. (8) and (9).

Although the physical meanings of $J_k(t)$ are generally not well interpreted due to their vanishing feature, they can still be used in determination of the asymptotic stress field. To this end, by choosing a small but finite radius R for the circular integration path Γ and denoting the '$J_{kR}(t)$-integrals' as alternatives for $J_k(t)$, we then rewrite Eqs. (11) and (12) as

$$J_{1R}(t) = \frac{\Lambda}{E}\left[R^{2\lambda_1+1}a(\beta)K^2_{\mathrm{I},\beta}(t) + R^{2\lambda_2+1}b(\beta)K^2_{\mathrm{II},\beta}(t)\right] \tag{13}$$

$$J_{2R}(t) = -\frac{2\Lambda}{E}R^{\lambda_1+\lambda_2+1}c(\beta)K_{\mathrm{I},\beta}(t)K_{\mathrm{II},\beta}(t) \tag{14}$$

With the cutoff radius R, $J_{kR}(t)$ turn out to be of finite values. The SIF's and, consequently, the corresponding stress field can then be determined should the integrals be properly evaluated. However, in order to have appropriate solutions for $K_{\mathrm{I},\beta}(t)$ and $K_{\mathrm{II},\beta}(t)$, it is required that R be taken in the region dominated by the asymptotic field. Singular behavior is thus always involved in the calculation. In finite element calculations, the discretized solutions will in general describe the behavior around the notch tip O more or less accurately, depending on the degree of local grid refinement and/or the adoption of special singular elements. Therefore, direct calculation of $J_{kR}(t)$ along Γ with numerical solutions appears to be difficult.

In addition to the proposed $J_{kR}(t)$-integrals, the SIF's for a notch tip can be calculated by using other types of contour integrals. For example, the H-integral was derived with the concept of Betti's reciprocal theorem and presented to compute either single- or mixed-mode SIF's in notched solids under quasi-static loads for specific notch angles (e.g. Carpenter, 1984; Sinclair et al., 1984; Babuska and Miller, 1984; Labossiere and Dunn, 1998, etc.). The integration is performed by using a set of particular complementary solutions satisfying the same field equations as the displacement and stress fields. By comparing with the H-integral, J_{kR} appears to be more straightforward in calculation since no extra complementary solutions are required. With this superiority, J_{kR} can then be directly evaluated in the postprocessor of the finite element code once the nodal displacements under deformation are solved.

4. Modified concept of path-independence

As described, the integration path Γ for $J_{kR}(t)$ is defined as a counterclockwise circular contour with center at the notch tip O and of small radius R. We assume the conditions when the notch edges are traction-free and body forces are neglected. By applying divergence theorem under the state of dynamic equilibrium, we can have the J_{kR}-integrals rewritten as

$$J_{kR}(t) = \int_{\Gamma_o}\left[Wn_k - \sigma_{ij}n_j\left(\frac{\partial u_i}{\partial x_k}\right)\right]\mathrm{d}s + \int_{C_1+C_2} Wn_k\,\mathrm{d}s + \int_A \rho\frac{\partial^2 u_i}{\partial t^2}\frac{\partial u_i}{\partial x_k}\,\mathrm{d}a \tag{15}$$

where ρ is the mass density; Γ_o is an arbitrary outer counterclockwise contour; C_1 and C_2 are the portions of line segments along the notch edges, which are enclosed by Γ_o and terminated at a distance R away from the tip O; A is the simply-connected domain bounded by Γ_o and the circular contour of radius R (which is shown as the shaded area in Fig. 1).

For the quasi-static case, the last term of Eq. (15) (i.e., the integral over domain A) vanishes. Furthermore, by considering the first component (i.e., $k = 1$) under the special condition when β equals 0, we note that the second term on the right hand side of Eq. (15) also vanishes. The integration then reduces to the conventional J_1-integral for crack problems. In such case, the value of integration remains unchanged along

any arbitrarily chosen outer contour Γ_o and this property is the well-known path-independence. With this property, Γ_o is usually taken to be far from the crack tip so that the singular behavior in the near-tip region can be neglected in the calculation. However, for the general condition when $\beta > 0$ and subjected to dynamic loads, extra integrals along the notch edges $C_1 + C_2$ and over the domain A must be included for both $J_{1R}(t)$ and $J_{2R}(t)$. The idea of path-independence hence needs to be modified by including these additional line and domain integrals.

Although the remote path Γ_o can be chosen arbitrarily, the extra line segments $C_1 + C_2$ should both be terminated in the near-tip region. Also, the domain A includes the near-tip region as R is chosen small enough to be inside the zone of the dominance of the asymptotic solution. With these portions of line and domain integrals, the asymptotic singular behavior is thus inevitably involved in the calculation. Cautious investigation for the numerical results is therefore necessary.

5. Numerical examples

In the following two subsections, two numerical example problems are presented. In the first problem, the $J_{kR}(t)$-integrals are evaluated and the associated features of the numerical results are investigated. In the second example problem, the generalized SIF's and the corresponding stress field are evaluated. Quadratic elements are used for displacement interpolation in the calculation. The transient analysis, neglecting damping effect, is performed by an unconditionally stable Newmark time integration scheme. No particular singular element is used throughout the study.

5.1. Problem 1—the $J_{kR}(t)$-integrals

The aim of this problem is to illustrate the proposed computation procedure and to evaluate the characteristics of the J_{kR}-integrals. Fig. 5(a) shows a plane strain elastic specimen containing a central wedge-shaped defect and subjected to dynamic combined loads $(\sigma(t), \tau(t))$. The combined loads $(\sigma_o\varphi(t), \tau_o\varphi(t))$ are given proportionally as step function of time $\varphi(t)$ (Fig. 5(b)).

The numerical study for this test problem is organized as follows. First, the effect of the local finite element approximation in the near-tip region is investigated. Second, calculations under a number of paths, each encircling different portions of the same finite element mesh, are carried out in order for examination of the property of generalized path-independence. Finally, the behavior of $J_{kR}(t)$ with respect to different selections of R is examined. Four instances of different notch angles (with β equal to 0, $\pi/4$, $\pi/2$, and $3\pi/4$ respectively) are considered in the following calculations. Note that the feasibility of our formulation for quasi-static problems has been demonstrated in the authors' previous work (Chang and Kang, 2002).

The finite element representation shown in Fig. 6 is used to analyze the specimen (e.g., of $\beta = \pi/2$). In the discretized model, the elements are progressively refined as they approach the notch tip. In order to investigate the effect of the local finite element approximations, several meshes are constructed by successive local h-refinements in the near-tip region, with the size of the tip-element ranging from '$l/25$' to '$l/250$'. Although not listed in detail here, the results obtained from the above different meshes show very good convergence.

Three integration paths, each enclosing different region of the above finite element mesh, are defined in the calculation to demonstrate the property of modified path-independence. The associated exterior contours Γ_o's of these paths are depicted in Fig. 7(a)–(c). As illustrated in Eq. (15), the calculation consists of three parts, including the integrations along Γ_o, the portion of the notch edges $C_1 + C_2$, and the domain A. The results of each part for $R = 4.22 \times 10^{-2} l$ m and $(\sigma_o, \tau_o) = (15, -20)$ kPa, at $t = 0.75$ s are shown in Table 1. It is observed that the integrations from $C_1 + C_2$ and A make significant contributions to the computation and thus account for the 'modified' property of path-independence. However, since the

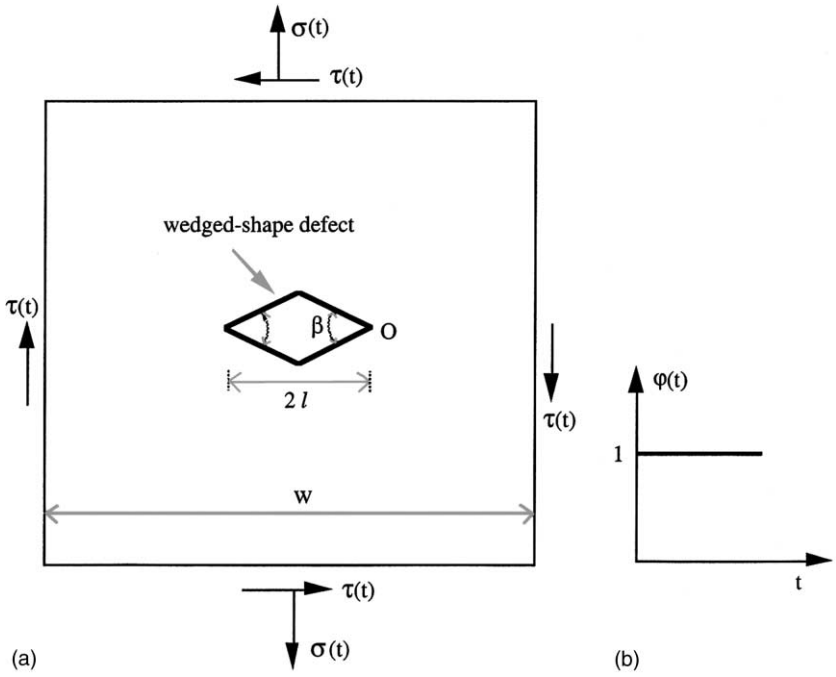

Fig. 5. (a) A homogeneous elastic body containing a wedged-shape defect. (b) Time function of the applied load.

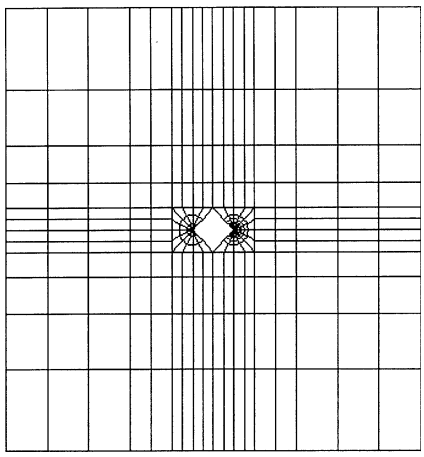

Fig. 6. The finite element model for the specimen in Fig. 5(a).

integrand in the last term of Eq. (15) is relatively non-singular, it is thus noted that the integration over A becomes less significant as Γ_o being chosen closer to the tip (e.g. path (c)). As a result, the solution from different paths in general yields very similar results of J_{kR}. Although the formulation is verified to be analytically path-independent in the modified sense, slight deviations among the results are observed because the dynamic equilibrium state is satisfied only weakly in the finite element computation.

Next, the behavior of J_{kR} with respect to various values of R is examined. Note that, in order to be able to use the proposed solution scheme, it is necessary that the values of R in the finite element calculation be

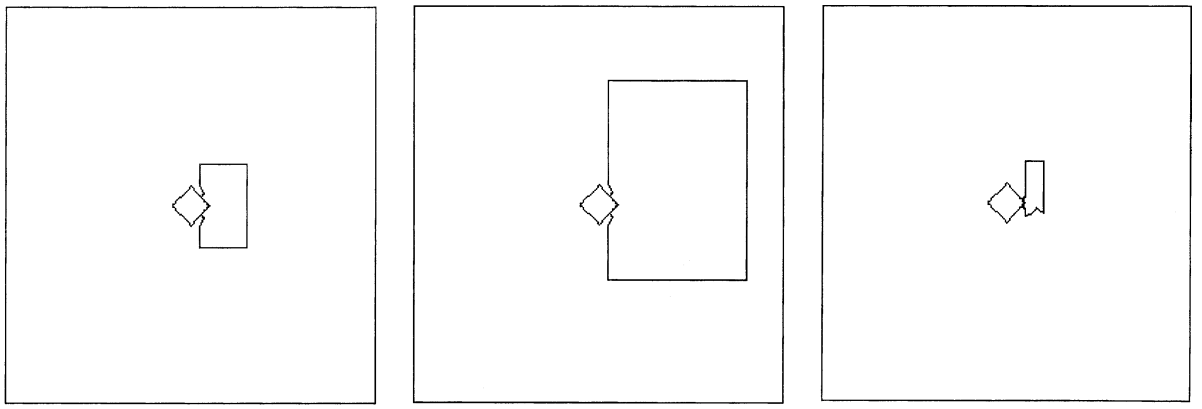

Fig. 7. Three integration paths for the J_{kR}-integrals.

Table 1
Path-independence for Problem 1 (Unit: 10^3 Pa m) (mixed-mode)

		$\int_{\Gamma_o}$	$\int_{C_1+C_2}$	$\int_A$	J_{1R}	$\int_{\Gamma_o}$	$\int_{C_1+C_2}$	$\int_A$	J_{2R}
Path									
$\beta = 0$	(a)	5.498	0	−0.654	4.844	−0.567	1.622	0.482	1.537
	(b)	7.802	0	−3.028	4.774	−2.698	1.622	2.605	1.529
	(c)	4.882	0	−0.040	4.842	1.433	0.107	0.002	1.542
$\beta = \pi/4$	(a)	9.751	−4.215	−1.616	3.920	1.729	0.554	0.467	2.750
	(b)	14.06	−4.215	−5.962	3.883	−1.301	0.554	3.550	2.803
	(c)	5.322	−1.197	−0.220	3.905	2.907	−0.178	0.003	2.732
$\beta = \pi/2$	(a)	7.100	−4.467	−1.120	1.513	1.265	−1.358	0.968	0.875
	(b)	9.674	−4.467	−3.718	1.489	−9.873	−1.358	12.09	0.859
	(c)	2.304	−0.669	−0.149	1.486	1.070	−0.428	0.230	0.872
$\beta = 3\pi/4$	(a)	3.926	−3.382	0.054	0.598	0.395	−1.220	0.979	0.154
	(b)	5.105	−3.382	−1.136	0.587	−1.052	−1.220	2.423	0.151
	(c)	0.948	−0.531	0.172	0.589	0.353	−0.199	0.005	0.159

$J_{1R} = \int_{\Gamma_o} + \int_{C_1+C_2} + \int_A$; $J_{2R} = \int_{\Gamma_o} + \int_{C_1+C_2} + \int_A$.
Note: $w = 30$ m, $l = 1.5$ m, $R/l = 4.22 \times 10^{-2}$, $E = 2.97$ MPa, $\nu = 0.3$, $\rho = 1384$ kg/m^3, $(\sigma_o, \tau_o) = (15, -20)$ kPa, $t = 0.75$ s (paths (a)–(c) are shown in Fig. 7(a)–(c) respectively).

taken small enough to be inside the zone of dominance of the asymptotic solution. By arbitrarily choosing the solution with respect to $R_o = 0.2 \times 10^{-2} l$ m as the reference, the normalized results of J_{kR}/J_{kR_o} for $(\sigma_o, \tau_o) = (15, -20)$ kPa, at $t = 0.75$ s are depicted as functions of the scaled cutoff radius $R/2l$ and shown in Fig. 8(a) and (b). The asymptotic slope of each curve extracted from the numerical fields, along with the analytical solutions for the order of the leading terms of J_{1R} and J_{2R} (as addressed in Eqs. (13) and (14)), are listed in Table 2. We observe that the computed results for the slope of $\ln(J_{2R})$ appear to be well consistent with the values of $\lambda_1 + \lambda_2 + 1$, with the errors to remain under 2%. On the other hand, substantial deviations between either $2\lambda_1 + 1$ or $2\lambda_2 + 1$ and the results of $\ln(J_{1R})$ are observed for $\beta = \pi/4$ and $\pi/2$ because the asymptotic solution of J_{1R} is governed by the appearance of both $r^{2\lambda 1+1}$ and $r^{2\lambda 2+1}$ under the mixed-mode

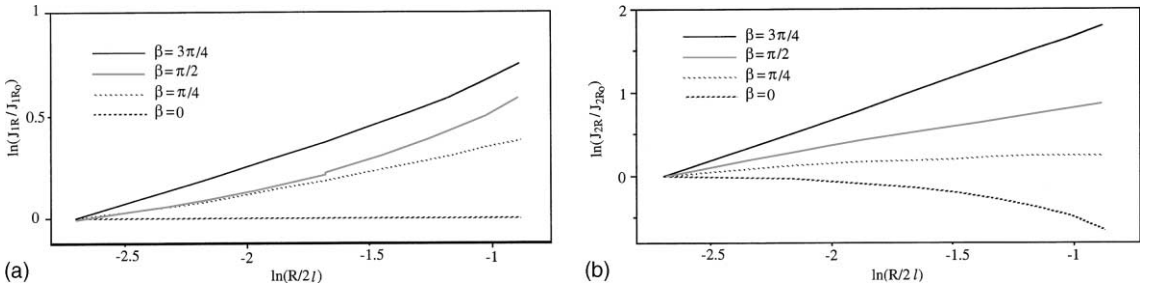

Fig. 8. The variations of J_{kR}/J_{kR_o} with respect to $R/2l$ for $(\sigma_o, \tau_o) = (15, -20)$ kPa, at $t = 0.75$ s.

loads. Nevertheless, the influence of $r^{2\lambda 2+1}$ becomes less significant when β increases so that the slope of $\ln(J_{1R})$ appears to be more close to the value of $2\lambda_1 + 1$, as is evident in the case of $\beta = 3\pi/4$, where the near-tip mechanical behavior is dominated by the mode I stresses.

The singular behavior of the dynamic J_{kR} appears to be similar to that in the quasi-static condition. For more discussions on the trend of the singularity with respect to the notch angle β, please refer to the authors' previous work (Chang and Kang, 2002).

Since the concept of the elastodynamic $J_{kR}(t)$-integrals for notches is originally presented in this paper, there is no analytical or numerical solution with which direct test of the above computation scheme can be carried out (except for the case $\beta = 0$). Nevertheless, the numerical results show that the integrals are path-independent (in a modified sense). Also, the computed values of the order of their leading terms in the asymptotic near-tip region are well consistent with those of the analytical solutions. The feasibility of the proposed integrals can thus be appropriately demonstrated by the observation and comparison.

5.2. Problem 2—the generalized SIF's

As demonstrated in the previous problem, the values of $J_{kR}(t)$ for a notch tip can be properly calculated from the finite element solutions. It is therefore possible to make use of the results of $J_{kR}(t)$ to determine the generalized SIF's $K_{I,\beta}(t)$ and $K_{II,\beta}(t)$ by using Eqs. (13) and (14). Consequently, the asymptotic stress field can then be evaluated.

In this problem, we first demonstrate the feasibility of the formulation by examining the numerical results of $K_{I,\beta}(t)$ and $K_{II,\beta}(t)$ computed from different selections of R. Again, we consider the plane strain specimen subjected to the combined loads $(\sigma_o\varphi(t), \tau_o\varphi(t))$ shown in Fig. 5. The generalized SIF's, resulting from the corresponding solutions of J_{kR}, associated with various values of R for various notch angles at $t = 0.75$ s are listed in Table 3 Note that, for $\beta = 0$, the SIF's (i.e., $K_{I,0}$ and $K_{II,0}$) are evaluated directly from J_k and essentially independent of R. The results, except those associated with $K_{II,3\pi/4}$, appear to be almost invariant

Table 2
The asymptotic slopes of $\ln(J_{kR})$ for Problem 1 (mixed-mode)

	$\ln(J_{1R})$	$\ln(J_{2R})$	$2\lambda_1 + 1$	$2\lambda_2 + 1$	$\lambda_1 + \lambda_2 + 1$
$\beta = 0$	0	0	0	0	0
$\beta = \pi/4$	0.154	0.164	0.01	0.319	0.165
$\beta = \pi/2$	0.176	0.450	0.089	0.817	0.453
$\beta = 3\pi/4$	0.341	0.991	0.347	1.604	0.976

Note: $w = 30$ m, $l = 1.5$ m, $E = 2.97$ MPa, $v = 0.3$, $\rho = 1384$ kg/m^3, $(\sigma_o, \tau_o) = (15, -20)$ kPa, $t = 0.75$ s.

Table 3
The results of $K_{I,\beta}$ and $K_{II,\beta}$ versus R for Problem 2 (mixed-mode) (Unit:10^4 Pa $m^{1/2}$)

$R/2l$ (10^{-2})		0.66	1.28	2.11	3.22
$\beta = 0$	$K_{I,0}$			3.174	
	$K_{II,0}$			−12.17	
$\beta = \pi/4$	$K_{I,\pi/4}$	5.235	5.242	5.248	5.242
	$K_{II,\pi/4}$	−16.99	−17.01	−17.33	−17.19
$\beta = \pi/2$	$K_{I,\pi/2}$	5.970	6.085	6.007	5.936
	$K_{II,\pi/2}$	−18.89	−18.39	−18.66	−18.70
$\beta = 3\pi/4$	$K_{I,3\pi/4}$	7.314	7.350	7.286	7.193
	$K_{II,3\pi/4}$	−10.23	−22.23	−34.81	−26.89

Note: $w = 30$ m, $l = 1.5$ m, $E = 2.97$ MPa, $v = 0.3$, $\rho = 1384$ kg/m^3, $(\sigma_o, \tau_o) = (15, -20)$ kPa, $t = 0.75$ s.

with respect to different selections of R, with maximum deviation to be under 2%, as anticipated. The exception observed for $K_{II,3\pi/4}$ is due to its non-singular behavior. In fact, $K_{II,3\pi/4}$ is trivial since it makes no contribution to the asymptotic stresses. Also, for the four instances of β considered in this problem, it is revealed that the value of the SIF's (again, except $K_{II,3\pi/4}$) increases as the notch angle increases. As an aside, it is suggested from our numerical results that the scale of R be within the range of $0.1l$ in order for accurate solutions of the SIF's.

Still, to further investigate the feasibility of the computation scheme, we reconsider the same specimen and impose the pure mode I and mode II loads separately (proportionally as step function of time $\varphi(t)$). The results of the generalized SIF's for $(\sigma_o, \tau_o) = (15, 0)$ kPa and $(\sigma_o, \tau_o) = (0, -20)$ kPa are shown in Tables 4 and 5 respectively. The numerical results appear to be well consistent with those evaluated from the mixed-mode solutions shown in Table 3, as expected. Note that the solution of $K_{II,3\pi/4}$ is not available numerically when the specimen is subjected to pure mode II load due to the appearance of the regular leading term $r^{1.604}$. As aforementioned, since the asymptotic mode II stress component is relatively negligible for notch angles greater than 0.57π, the feature of $K_{II,\beta}(t)$ is therefore insignificant in such cases.

The calculated transient dynamic SIF's for $\beta = \pi/4$ subjected to the step combined load $(\sigma(t), \tau(t)) = (15\varphi(t), -20\varphi(t))$ kPa are shown in Fig. 9. The results are normalized with respect to the quasi-static SIF's (i.e., $(K_{I,\pi/4})_s$ and $(K_{II,\pi/4})_s$) so that the dynamic amplifying effect can be observed. The figure reveals that, while the maximum dynamic $K_{I,\pi/4}(t)$ can be 2.4 times of $(K_{I,\pi/4})_s$, the peak for $K_{II,\pi/4}(t)$ reaches up to 3.7 times of its static value in this case.

Table 4
The results of SIF's versus β for Problem 2 (mode I)

β	0	$\pi/4$	$\pi/2$	$3\pi/4$
$K_{I,\beta}$ (10^4 Pa $m^{1/2}$)	3.253	5.187	6.020	7.229
$K_{II,\beta}$ (10^4 Pa $m^{1/2}$)	0	0	0	0

Note: $w = 30$ m, $l = 1.5$ m, $E = 2.97$ MPa, $v = 0.3$, $\rho = 1384$ kg/m^3, $(\sigma_o, \tau_o) = (15, 0)$ kPa, $t = 0.75$ s.

Table 5
The results of SIF's versus β for Problem 2 (mode II)

β	0	$\pi/4$	$\pi/2$	$3\pi/4$
$K_{I,\beta}$ (10^4 Pa $m^{1/2}$)	0	0	0	0
$K_{II,\beta}$ (10^4 Pa $m^{1/2}$)	−12.43	−17.34	−18.83	–

Note: $w = 30$ m, $l = 1.5$ m, $E = 2.97$ MPa, $v = 0.3$, $\rho = 1384$ kg/m^3, $(\sigma_o, \tau_o) = (0, -20)$ kPa, $t = 0.75$ s.

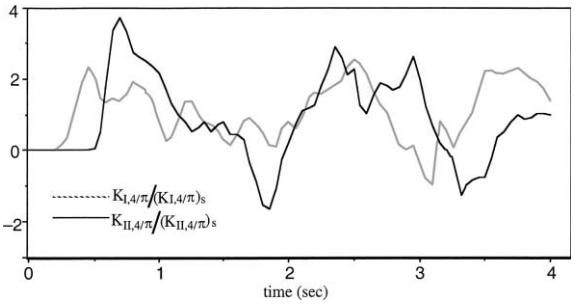

Fig. 9. The calculated transient dynamic SIF's for $\beta = \pi/4$ (mixed-mode).

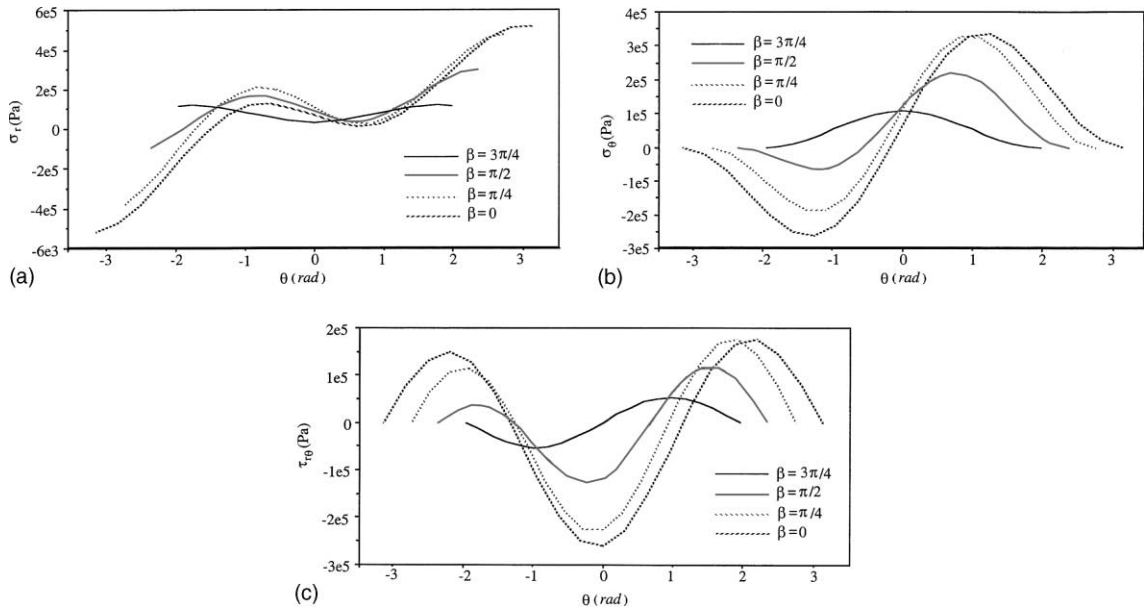

Fig. 10. (a)–(c) The asymptotic stress field under $(\sigma_o, \tau_o) = (15, -20)$ kPa at $r = 2.33 \times 10^{-2} l$ when $t = 0.75$ s.

By substituting the generalized SIF's into Eqs. (1)–(3), the asymptotic stress field can then be appropriately calculated. The circumferential distribution of the stresses for different notch angles under the combined load $(\sigma_o, \tau_o) = (15, -20)$ kPa at, say, $r = 2.33 \times 10^{-2} l$, when $t = 0.75$ s are evaluated and shown in Fig. 10(a)–(c). The results show that the strength of stress concentration decreases essentially as the value of β increases. Such behavior is consistent with that of the analytical solutions, where the order of singularity becomes weaker as β increases. It is also observed that the contribution from the mode II stress components become less significant as β increases. As a matter of fact, for the case of $\beta = 3\pi/4$, the stresses are observed to be almost dominated by the mode I components, as anticipated.

Although there is no analytical or numerical solution for direct verification of the above calculation (except for the case $\beta = 0$), the validity of the formulation for the generalized SIF's can be demonstrated by addressing the following two points. First, the numerical results of $K_{I,\beta}(t)$ and $K_{II,\beta}(t)$ appear to be invariant with respect to different selections of the cutoff radius R, as anticipated by Eqs. (13) and (14). Also, the computed values of the mixed-mode SIF's are well consistent with those evaluated from the pure mode I and mode II loads, as expected.

6. Conclusions

A numerical procedure is provided for calculation of the elastodynamic asymptotic mixed-mode stress field for plane elastic problems containing a stationary notch tip. To this end, we first define a pair of contour integrals termed $J_{kR}(t)$, along with a pair of the generalized dynamic SIF's $K_{\mathrm{I},\beta}(t)$ and $K_{\mathrm{II},\beta}(t)$. The relationship between $J_{kR}(t)$ and the SIF's is then analytically derived and expressed in Eqs. (13) and (14). The values of the coefficients $a(\beta)$, $b(\beta)$, and $c(\beta)$ appear to be functions of the notch angle β only. In principle, once the $J_{kR}(t)$-integrals are evaluated, the generalized SIF's and, consequently, the dynamic asymptotic near-tip mixed-mode stress field can then be completely determined.

In order to properly characterize the near-tip behavior, it is required that the cutoff radius R be taken small enough so the integration contour for $J_{kR}(t)$ be inside the region dominated by the asymptotic field. Therefore, direct calculation of the $J_{kR}(t)$-integrals with finite element solutions appears to be difficult. Nevertheless, the integrals are shown to be path-independent in a modified sense. The integration can thus be alternatively carried out by including three parts, i.e., an arbitrarily chosen outer contour Γ_{o}, the line segments along the notch edges $C_1 + C_2$, and the domain A. With this property, accurate solutions can be achieved without using any particular singular elements. The feasibility of our formulation is then demonstrated in the numerical examples via detailed investigations of the computed asymptotic behavior. Also, it is verified numerically that the results of $K_{\mathrm{I},\beta}(t)$ and $K_{\mathrm{II},\beta}(t)$ are actually insensitive to different selections of R. In summary, the proposed numerical scheme can be used to investigate the dynamic amplifying effect in the near-tip stress field.

Acknowledgement

This work has been partially supported by National Science Council grant no. NSC90-2211-E-008-040 to National Central University.

References

Awaji, H. et al., 1986. The variation of the stress singularity at the notch tip as notch angle and radius of curvature. Comp. Struct. 22 (1), 25–30.

Babuska, I., Miller, A., 1984. The post-processing approach in the finite element method—Part 2: the calculation of stress intensity factors. Int. J. Num. Meth. Eng. 20, 1111–1129.

Bogy, D.B., 1972. The plane solution for anisotropic elastic wedges under normal and shear loading. J. Appl. Mech. 39, 1103–1109.

Budiansky, B., Rice, J.R., 1973. Conservation laws and energy-release rates. ASME, J. Appl. Mech. 40, 201–203.

Carpenter, W.C., 1984. Calculation of fracture parameters for a general corner. Int. J. Fract. 24, 45–58.

Chang, J.H., Chen, C.B., 1998. Calculation of the elastodynamics energy parameter for a plane crack prior to kinking. ASCE, J. Eng. Mech. 124 (3), 268–276.

Chang, J.H., Kang, L.K., 2002. Evaluation of the stress field around a notch tip using contour integrals. Int. J. Eng. Sci. 40, 569–586.

Eischen, J.W., 1987. An improved method for computing the J_2 integral. Eng. Fract. Mech. 26 (5), 691–700.

Hellen, T.K., Blackburn, W.S., 1975. The calculation of stress intensity factors for combined tensile and shear loading. Int. J. Fract. 11, 605–617.

Herrmann, A.G., Herrmann, G., 1981. On energy release rates for a plane crack. ASME, J. Appl. Mech. 48, 525–528.

Knowles, J.K., Sternberg, E., 1972. On a class of conservation laws in linearized and finite elastostatics. Arch. Rat. Mech. Anal. 44, 187–211.

Labossiere, P.E.W., Dunn, M.L., 1998. Calculation of stress intensities at sharp notches in anisotropic media. Eng. Fract. Mech. 61, 635–654.

Nishioka, T., Atluri, S.N., 1983. Path-independent integrals, energy release rates, and general solutions of near-tip fields in mixed-mode dynamic fracture mechanics. Eng. Fract. Mech. 18 (1), 1–22.

Peng, X., 1986. On stress singularities at tips of plane notches. Mech. Res. Com. 13, 173–178.

Sinclair, G.B., Okajima, M., Griffin, J.H., 1984. Path independent integrals for computing stress intensity factors at sharp corners in elastic plates. Int. J. Num. Meth. Eng. 20, 999–1008.

Williams, M.L., 1952. Stress singularities resulting from various boundary conditions in angular corners of plates in extension. J. Appl. Mech. 19, 526–528.